Breadboard Testing of a HiPeR Inflatable Radiator (HiPeR INFRA)

Tom de Groot[1] and Boudewijn Schwieters[2]
Airbus Defence and Space Netherlands B.V., P.O. Box 32070, 2303 DB Leiden, The Netherlands

and

Roel van Benthem[3], Johannes van Es[4] and Aswin Pauw[5]
Royal Netherlands Aerospace Centre (NLR), P.O. Box 90502, 1006 BM Amsterdam, The Netherlands

With a twenty times higher thermal conductivity per unit mass than aluminium, pyrolytic graphite (PG) offers great potential in the application to spacecraft thermal control systems. Over the last years, Airbus Defence and Space Netherlands (Airbus DS NL) has been developing thermal control applications for this material. The patented High Performance Radiator (HiPeR) uses the PG to efficiently spread the heat from a heat source over a large radiative area. Recently, Airbus DS NL and the Royal Netherlands Aerospace Centre (NLR) have been working on a HiPeR Inflatable Radiator (INFRA) application. This concept consists of a HiPeR radiator and a single phase fluid loop. Flexible tubing enables the radiator to be rolled up to a small stowed volume. Once in orbit, the system pressure is increased, triggering the radiator to unroll and maintain its shape over the mission lifetime. Heat is supplied via the same fluid tube that gives the radiator its shape, making use of a dedicated mini-pump. To validate the functional design, a breadboard model has been made. Deployment and thermal performance have been tested successfully. Based on the measured data, the thermal performance of the breadboard INFRA system operating at a 45 °C root temperature in a space environment with a sink temperature of -270 °C would be approximately 300-325 W/m^2, corresponding to a radiator efficiency of approximately 60%. The two-sided surface of the breadboard INFRA system has a total surface area of 0,8 m^2. The performance is deemed to be competitive, especially considering the mass-to-power (expected <10 kg / kW after a design iteration) and small stowed volume of such a system. Additionally, a small-scale breadboard test of protection measures against micro-meteoroids and orbital debris (MMOD) has yielded promising results. The revised design, with MMOD shielding in the form of bi-stable metal strips, has a resulting probability of no penetration of the kapton fluid tubing in the breadboard INFRA model of 0,9 over a lifetime of 15 years. The adverse effects of MMOD shielding are substantial (estimated thermal impact 25-50%, mass impact 20-30%, stowed volume 10-20%) however there is ample room for optimization of the design and manufacturing methods.

Nomenclature

BB	=	Breadboard
BLM	=	Ballistic Limit Models
DRAMA	=	Debris Risk Assessment and Mitigation Analysis
ESA	=	European Space Agency
FR	=	Foil Radiator
FRA	=	Foil Radiator Assembly

[1] Sales Engineer / Project Manager, Mechanical and Thermal Products, t.de.groot@airbusds.nl.
[2] Test Engineer, Assembly, Integration and Testing
[3] Senior Research Manager, Energy Management/Thermal Control, roel.van.benthem@nlr.nl.
[4] Principal Scientist Thermal Control Group, johannes.van.es@nlr.nl.
[5] Senior Engineer, Thermal Control, aswin.pauw@nlr.nl.

FRF = FR Fixation
FRRS = FR Roll Support
HDRM = Hold-Down and Release Mechanism
HiPeR = High Performance Radiator
HT = Heat Transfer
INFRA = Inflatable Radiator
IR = Infrared
MIDAS = MASTER-based Impact Flux and Damage Assessment Software
MMOD = Micro Meteoroid and Orbital Debris
NLR = Royal Netherlands Aerospace Centre
PA = Pump Assembly
PG = Pyrolytic Graphite
PNP = Probability of No Penetration
RS = Radiator System
TRL = Technology Readiness Level

C_p = specific heat
$\dot{m}$ = mass flow
η = efficiency
Q = power
T = temperature
α, θ = angle

I. Introduction

First conceptualized in 2013, the High Performance Radiator (HiPeR)[1-3] and dedicated mini-pumps have been combined in 2016 in the concept of a HiPeR Inflatable Radiator (INFRA). This concept is a lightweight inflatable radiator system analogous to a butterfly wing (see Figure 1), where fluid provides the internal pressure to unfold the structure and provides heat transport from the payload to the radiating surface.

Figure 1. Inspiration from nature: blood circulation through butterfly wings has a dual function: unfolding (by increasing blood pressure in the veins) and thermal management (in this case heating by basking in the sun).

The need for INFRA is outlined in section II. An overview of the system is presented in section III, with details provided in section IV. The current status (results of breadboard testing and lifetime feasibility) is included in section V. Sections VI and VII provide a brief future outlook and a conclusion.

II. The need for an Inflatable Radiator (INFRA)

Currently, satellites are starting to become limited in their payload capacity by the heat rejection capability which is constrained by the exterior surface area of the spacecraft. A deployable/inflatable system has the potential to extend the surface available for heat rejection and thus allow further growth of satellite platforms. The INFRA solution offers more flexibility in terms of design and integration/testing at a lower mass than conventional aluminium radiator panels. The INFRA concept offers a very compact stowed volume that could conveniently be stowed alongside a spacecraft's solar arrays or in between deployable antenna reflectors. The concept is applicable to all types of missions without depending on details of the spacecraft layout such as the presence, location and size of its solar arrays, antennas and other appendages. The integration of functions (the use the internal pressure of a cooling system to provide the pressure for inflation) leads to a mass reduction. Also, INFRA offers reduced cost because of its simplicity (reduced number of mechanisms such as hold-down and release), simpler manufacturing techniques (no autoclave baking of sandwich panels with embedded heat pipes, simpler non-destructive inspections or none at all) and because of low the mass and small stowed volume there will be less need to optimise its size. To provide a high epsilon/low alpha outer surface, flexible white paint can be applied to the radiating surface.

III. INFRA High-Level System Description

The Radiator System (RS) is composed of two subsystems: the Pump Assembly (PA) and the Foil Radiator Assembly (FRA). The PA is designed to circulate a fluid (single phase) with redundant mini-pumps to support heat transport from the payload to the Foil Radiator (FR). The fluid is used to transport heat from the payload to the FR and also to apply the pressure used for deployment of the FR. The function of the FRA is to stow and deploy the FR and consists of a Hold Down and Release Mechanism (HDRM) and Foil Radiator Roll Support (FRRS). The Foil Radiator Fixation (FRF) fixates the base of the FR to the spacecraft wall. A system overview of the RS is included in Figure 2. The hover disk and the PA interface supports were only included to support handling and simulation of zero-g deployment during the breadboard tests and are not part of the baseline design.

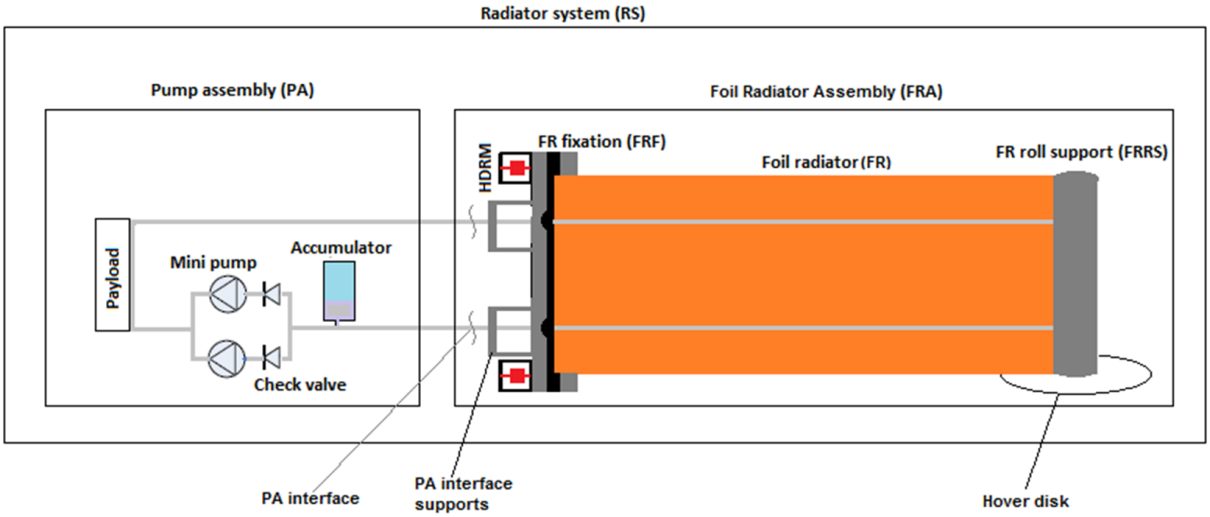

Figure 2. Radiator System overview

The baseline design is inspired by a butterfly wing (see Figure 1) and can also be compared to a "party-whistle". The baseline design is not retractable; this may be included in future developments (see section VI). The RS design properties are elaborated in Table 1.

Table 1. Design properties of the Radiator System (RS)

RS property	Elaboration
Scalability	FR surface area and accumulator size can be scaled for additional heat dissipation
(Re-)stowability	FR can be rolled-up and stowed into a small volume.
Single deployment	HDRM and FR are designed for single deployment. Multiple re-deployments require a design iteration (see section VI).
Double sided radiator	Maximum radiative area by using both sides. Various surface coatings can be used to control the radiative area and emissivity.
Redundancy	Tubes and pumps are high-risk components and therefore multiple pumps & fluid loops can be used redundantly.
High fin efficiency	Use of HiPeR enables high fin efficiency. Spacing of the fluid tubing can be varied for optimisation of the efficiency.
Mass-to-power	The target mass-to-power ratio of for INFRA is 10 kg/kW, or 5 kg/kW per subsystem for the PA and FRA (equally distributed for simplicity). It is assumed that the mass of the PA and FRA scale with size/power.
Modularity and validation	The heat transfer fluid can be routed from the payload to the FR, which allows a modular design adjustable to the payload and interface with the PA. The system performance should be validated on system level.
Integration	The PA requires a small volume inside the spacecraft between payload and the spacecraft wall. The FRA can be integrated with the spacecraft wall.
TRL level after BB testing	TRL3 / TRL4

A. Performance of the Radiator System

The performance of the RS was estimated using ESATAN ThermXL and verified/correlated with test data. The performance of the RS before and after verification/correlation with test results can be found in Table 2.

Table 2. Performance of Radiator System (RS)

	Performance parameter	Design	Breadboard model
Pump Assembly (PA)	Heat transfer (HT) fluid	Galden HT 55	Galden HT 55
	Nominal mass flow ($\dot{m}$)	27,5 g/s	27 – 36 g/s
	Deployment pressure FR tubing	1,5 bar	0,5 – 2,0 bar
	FR Tubing configuration	Single fluid loop, single pass	Single fluid loop, single pass
	Pumps	Two parallel mini centrifugal pumps with check-valves*	Two parallel mini gear pumps without check valves
	Pressure limit	3 bar	3 bar
	Payload (heater) power (Q)	400 W	0 – 200 W
Foil Radiator Assembly (FRA)	Stowing volume	0,016 m^3	0,006 m^3
	Total radiator surface area	0,8 m^2	0,8 m^2
	Emissivity FR	0,83 (white paint)	0,84 (no paint)
	Root temperature (T_R)	30 °C – 45 °C	45 °C
	Fin efficiency (η)	50 ± 10%	55 – 60%
	Heat dissipation in deep space (Q_{FR})	270 W (337 W / m^2)	240 – 260 W (300 – 325 W/m^2)
	Stiffness deployed FR	0,14 N/m	0,26 – 0,32 N/m

B. Comparison to conventional deployable radiator

The main advantages of INFRA compared with a conventional deployable radiator are its stowability, its mass-to-power ratio and the simplicity of manufacturing and integration:

- Stowability is enabled by flexibility: stowing a (large) radiator surface in a smaller volume alongside other spacecraft components (e.g., solar arrays, antenna reflectors).
- The targeted mass-to-power ratio is superior to conventional (aluminium) deployable radiators.
- Simple manufacturing techniques allow for a lower cost manufacturing and non-destructive inspection compared to (for example) carbon fibre panels.
- The relatively simple deployment by inflation limits the required supporting mechanisms and hold-down points required for integration with the spacecraft.

IV. INFRA Detailed System Description

A. System overview

As described in section III, the RS is composed of the PA and the FRA subsystems. These were modelled, manufactured and tested on breadboard level. The RS breadboard model can be seen in Figure 3.

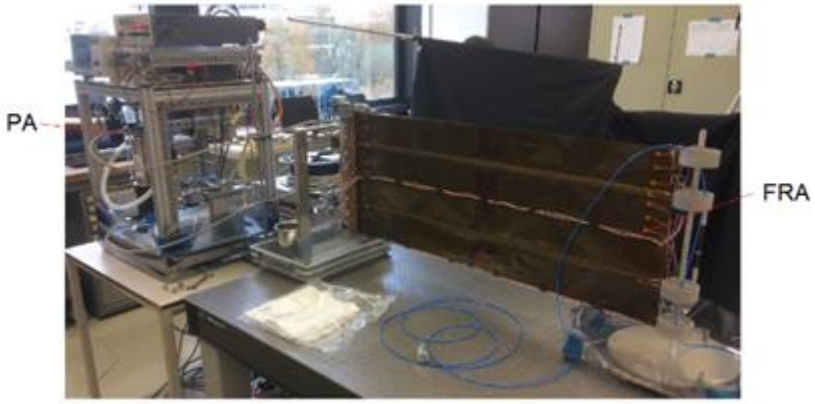

Figure 3. RS breadboard model

* Check valves prevent counter flow between the pumps.

B. Pump Assembly

The main purpose of the PA is to transport heat by circulating a fluid and to maintain the system pressure required to keep the FRA deployed in an ambient environment (1,0 to 2,5 bar). The selected heat transport fluid (Solvay Solexis Galden HT) is qualified for use in single-phase mechanical pumped fluid loops in space applications[4-6]. Galden HT fluids are not sensitive to radiation, which makes these fluids very stable throughout the mission lifetime. Galden HT55 was selected for its boiling point of 55˚C at ambient pressure. However, a system pressure slightly higher than ambient pressure was needed to prevent the fluid from boiling below 60˚C and to keep the FRA fully deployed both in air (ground test) and in vacuum (space). A system pressure of about 2 bar was maintained by heating the fluid in the accumulator to around 80˚C (see Figure 4).

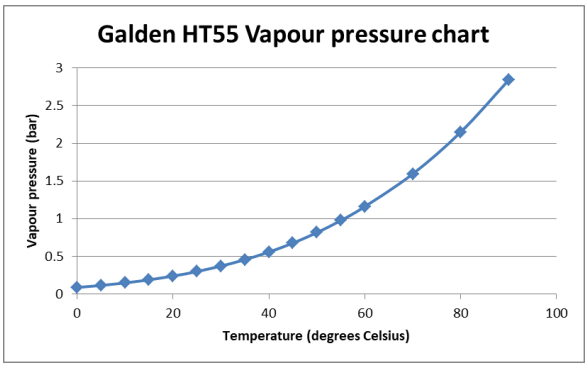

Figure 4. Vapour pressure of Galden HT55

The amount of heat Q [W] transported by the fluid is a function of the mass flow $\dot{m}$ [kg/s], the specific heat C [J/kg/K] and the temperature increase ΔT of the fluid [K].

$$Q = \dot{m} \cdot C \cdot \Delta T \qquad (1)$$

The design of PA includes two redundant commercial mini-gear pumps (type TCS MGD1000F) and a heat-controlled two-phase accumulator (Swagelok sample cylinder, volume 300 cm^3). See Figure 5 for a schematic representation of the thermo-hydraulic loop used for the PA. The PA outlet and inlet tubes were interfacing with the FRA. A flow meter (Rheonik RHM03) was added for flow measurements and a cartridge heater (OD 6 mm, power 400 W at 60 V) was included to simulate the heat dissipated by the payload.

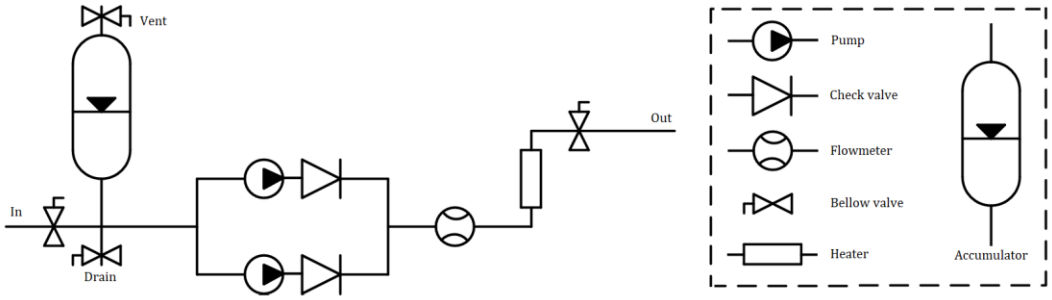

Figure 5. Schematic layout of the pump assembly

See Figure 6 for the layout and a photograph of the Pump Assembly. The two-phase accumulator has a 70% lower mass than a typical bellows accumulator in mechanically pumped fluid loops. This mass advantage adds to the technical and economic competitiveness of pumped fluid loops.

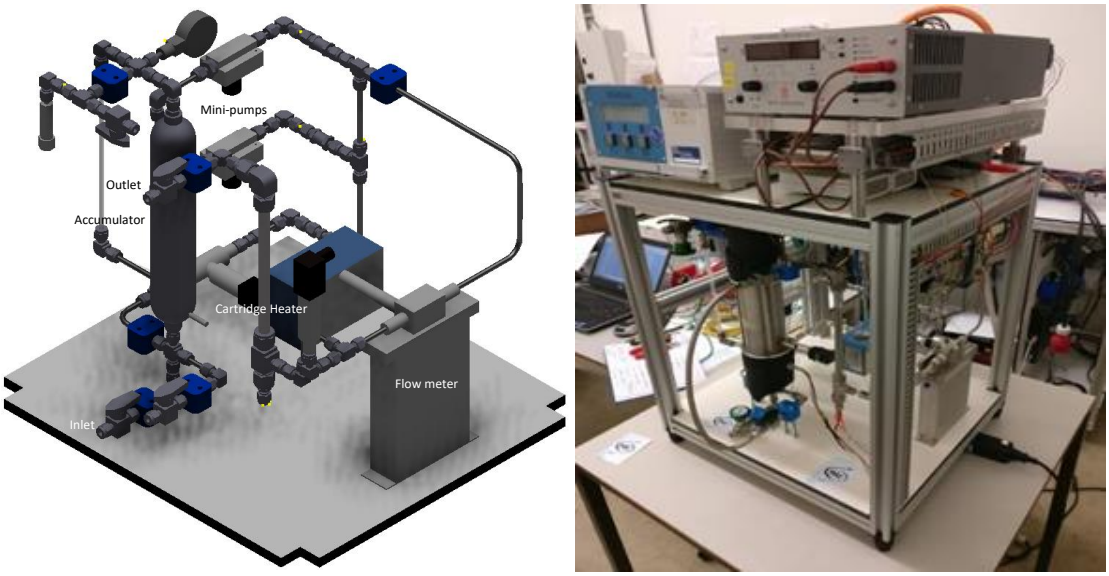

Figure 6. Layout and photograph of the Pump Assembly (PA)

The commercial mini-pump (Figure 7) has been ruggedized with Swagelok fluid connections. In the future, the mini gear-pumps may be replaced by multi-parallel micro-pumps (see Figure 8) which are under development at NLR for low-power units for CubeSat applications. An advantage of having multiple micro-pumps is that a single failure would not lead to a complete loop failure but only to degraded performance. Also the drive electronics are simple and low cost. Typical specifications for a 5-unit arrangement are a power consumption of 600 mW, a flowrate of 15 mL/min, a pressure head of 50 mbar and a mass of 100 g (excluding electronics).

Figure 7. TCS MGD1000F mini-gear pump as used for the Pump Assembly

Figure 8. Multi-parallel micro-pump under development at NLR

C. Foil Radiator Assembly

The FRA consists of four subsystems, which will be explained in this section:

- Foil Radiator (FR): heat transportation and heat dissipation to surrounding/space
- Foil Radiator Fixation (FRF): fixation of the FR to the spacecraft wall, minimization of heat leaks
- Hold-Down and Release Mechanism (HDRM): hold down of FRA during launch and release for operation
- Foil Radiator Roll Support (FRRS): roll up support and interface between FR and HDRM

The HiPeR baseline design includes a heat pipe and a fin length (maximum distance between heat pipe and edge of radiator) of 10 cm. The HiPeR baseline demonstrates a fin efficiency in vacuum and at $T = 3K$ of >80%. For INFRA, the fin length was maintained and a reduction in efficiency to >50% was accepted to provide a baseline design that can be optimized by reducing the tube spacing. The width of the FR was therefore selected to be 40 cm, existing of two sheets of HiPeR with a 5-mm isolator in between to improve test and modelling quality. The length of the radiator (1 m) was selected to have an easy-to-scale parameter and to have an FR that can satisfy low-power requirements and demonstrate deployment and thermal functionality. The tubing extends from the FR such that

thermal load was equally distributed and such that the radiator was convenient to roll up and interface with the FRRS. The tubing was embedded with an additional strip of HiPeR that was bonded onto the main foil. Multiple interface designs were evaluated, optimising for maximum contact area and minimum delamination/degradation of the interface. The foil radiator was manufactured at room temperature using simple tooling: scissors and (easy to apply) pressure-sensitive adhesive. Several manufacturing images are shown in Figure 9.

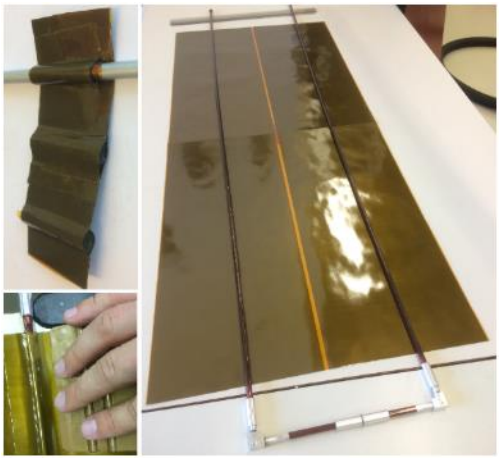

Figure 9. Manufacturing of FR

The thin-walled polyimide tubing has dimensions very similar to a drinking straw. The tubing was interfaced with 90-degree aluminium connectors to return the flow of heat transfer fluid at the end of the FR. Simply bending the tube would create a fold that could limit the flow. Several concepts have been evaluated for the connectors (see Figure 10). Concept 3 was selected as the most robust design. The principle of concept 3 was applied in both the PA/FR interface and the corner connectors. The corner connectors were equipped with a Vespel® interface to the FRRS, to thermally isolate the tubing from the FRRS.

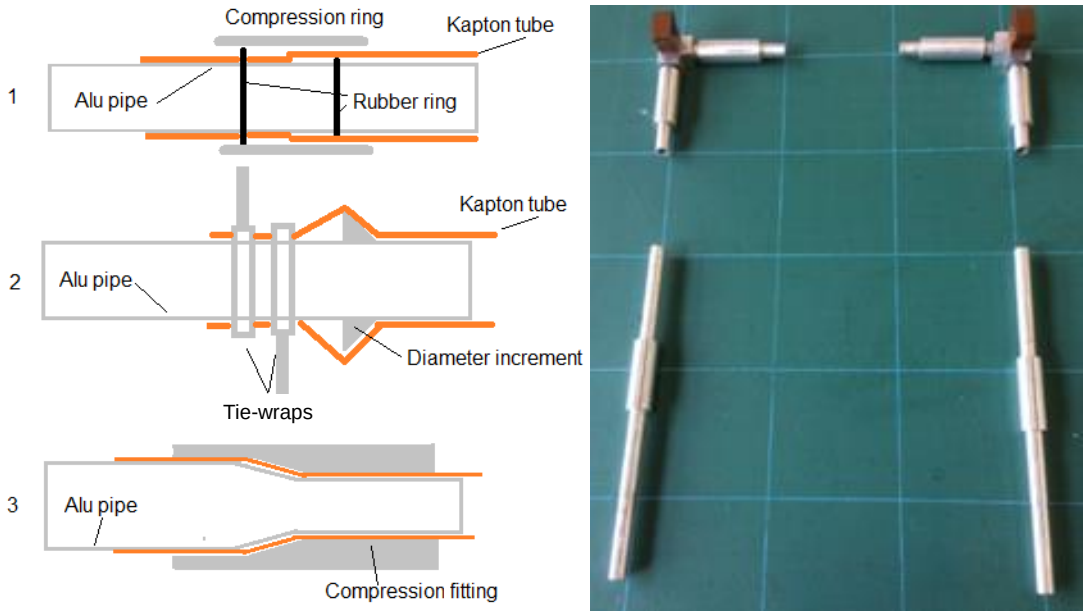

Figure 10. Connector concepts (left, not to scale), Concept 3 as used in BB model (right)

The function of the FRRS is to facilitate the interface of the tubing with the FR and to facilitate the roll-up the FR (see Figure 11). The FRRS was rolled over the length of the FR, creating a robust package that can sustain typical handling and launch loads. The four rollers were connected by a central beam equipped with endfittings that interface with the HDRM. The rollers have been 3D printed using Scalmalloy®. In the future, the rollers could be manufactured from plastics/composites to reduce the system mass, thereby reducing launch loads on the RS.

The HDRM holds down the FRRS endfittings on both sides of the FR and prevents movement (translation and rotation) of the FRRS during launch. The endfittings were held down inside a spring-loaded endfitting with a preloaded Dyneema® thread. Dyneema was selected for its high strength and low melting temperature. Preloading was done by rotating a circular disk using a wrench and locking it with a pin or a bolt. During deployment the thread was cut using a redundant spring-driven resistor (1Ω) mounted in a high temperature-resistant Vespel cylinder. The HDRM can be seen in Figure 12.

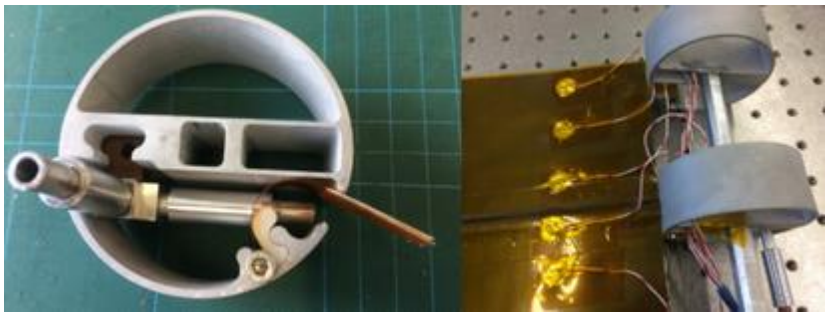

Figure 11. 3D Roller design (left), FRRS integrated with FR (right)

Figure 12. Hold-Down and Release Mechanism (HDRM, left), Foil Radiator Fixation (FRF, right)

The FRF has been used to clamp the FR and sustain handling or launch loads as well as thermally isolate the heat within the FR from the spacecraft wall (see Figure 12). Layers of cork provide thermal isolation and put sufficient pressure onto the FR to clamp it, but without damaging it. Two interface supports have been created for handling loads and isolation while testing the RS. The FRF consists of aluminium beams and stainless steel bolts for the BB tests; this can be optimized for mass and for integration with (honeycomb) spacecraft wall panels.

V. INFRA Current Status

As per the beginning of 2019, a system breadboard test has been conducted on the Radiator System (Pump Assembly and Foil Radiator Assembly), see section V.A. In addition, a small-scale breadboard test of protection measures against micro-meteoroids and orbital debris (MMOD) has been conducted (see section V.B).

A. System Breadboard Testing

The system has been tested on deployment and thermal performance. Deployment of the FRA has first been tested separately, followed by a thermal performance test of the RS and a combined deployment and thermal performance test of the RS. The deployment rig used to perform a simulated zero-G deployment test is shown in Figure 13. The honeycomb hover disk was supported by air bearings which allow a near-frictionless motion (translational and rotational) of the FRRS. A flat optics platform was used as ground surface for deployment.

1. Deployment test of Foil Radiator Assembly (FRA)

The FRA deployment test was performed using pressurized air instead of the heat transport fluid. Four absolute pressure levels were used: 1,5 / 2,0 / 2,5 / 3,0 bar. The results of the tests showed no complications, however the abrupt release of the pressurised FR resulted in a wider sweep of the FRRS on the deployment table than expected. During the RS test (see section V.A.3), the pressure was built up much more gradually and therefore the deployment occurred slower. As expected, the deployment speed reduced with reducing pressure.

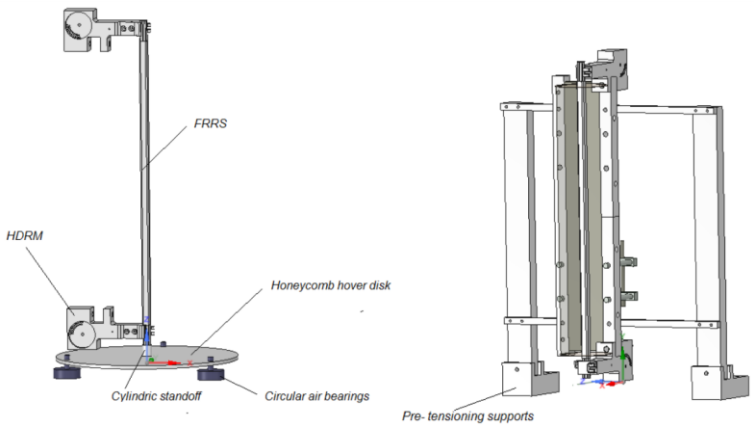

Figure 13. Deployment rig for system breadboard testing

2. Thermal performance test of Radiator System (RS)

For the thermal performance test, the FR was fully deployed and the air bearings in the hover disc were not pressurized. The setup is shown in Figure 14. The heat transfer fluid (deionized water) was circulated using a low volume flow aquarium pump. The mass flow was measured with a weighing scale at the exit of the FR. The measured mass flow was 8 ± 0,1 g/s. A proportional integrator differentiator regulator was coupled with a thermocouple and a heater element for temperature control in the thermal bath. The inflow temperatures were controlled at 30 / 45 / 60 °C ± 1 °C. An optical cloth barrier was installed to facilitate infrared (IR) imaging. The locations of the thermocouples (T-Type) are shown in Figure 15.

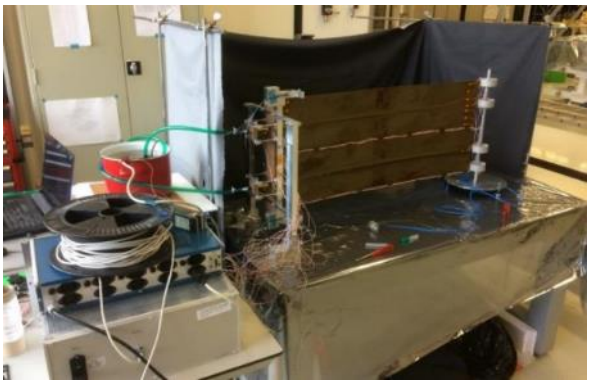

Figure 14. FR Thermal test setup

The power output (Q_{out}) of the FR was calculated on different test dates and room temperatures using equation (1) on page 5:

$$Q_{out} = \dot{m} \cdot C_{p_{wat}} \cdot \Delta T_{01-19}$$

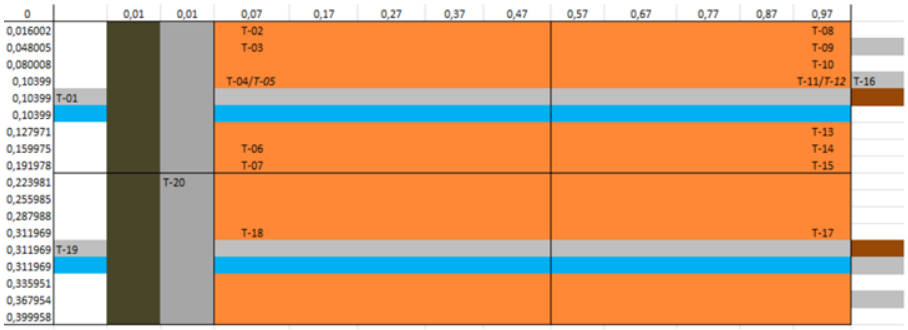

Figure 15. Thermocouple locations

Where $\dot{m}$ and $C_{p_{wat}}$ are the mass flow and specific heat of the deionized water, respectively and ΔT_{01-19} is the temperature difference measured between thermocouples T-01 and T-19. Due to the highly conductive FR, the time required to reach steady state was mostly dependent on the water, which takes a few minutes to reach the required temperature using a 1000W heater. The estimated heat outputs are shown in Figure 16. Heat was extracted from the FR by a combination of convection (natural and forced) and radiation. No cold plate was used. To identify the influence of natural convection, the FR was positioned on the table vertically and horizontally in separate test runs. In the horizontal position, the mass flow ($\dot{m}$) was slightly lower, resulting in a lower power output (Q_{out}). The vertical setup has been used as the main setup for the RS test.

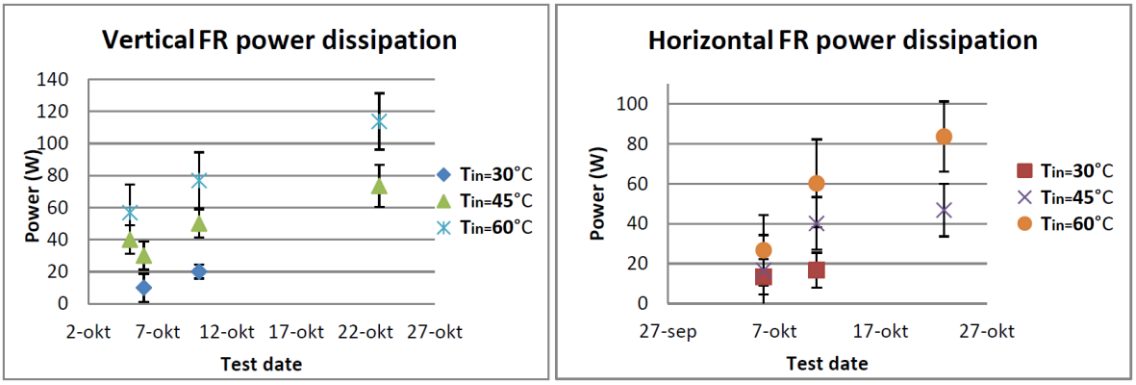

Figure 16. Heat output for various inflow temperatures on different test dates ($T_{env} = 22 \pm 1°C$)

The results show a rather large variation of the heat output on different days. This could be due to variations in the facility temperature (not measured), the temperature of the adhesive (which influences conductance of the thermal interface) or disturbed natural convection in the (large) test facility.

3. Combined deployment and thermal performance test of Radiator System (RS)

Deployment tests on the RS were conducted to determine the deployment behaviour with the pressure as generated by the PA. The test setup is shown in Figure 17. The vertical position has been selected for its higher heat output (see Figure 16) and ease of deployment.

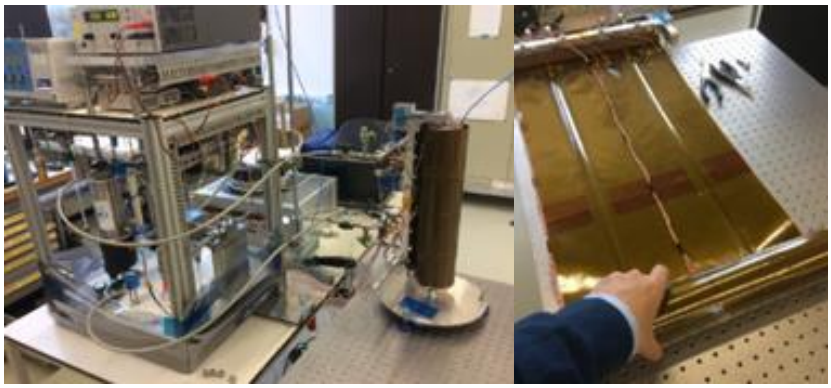

Figure 17. RS deployment test setup (left), rolling up the FR (right)

The test results are comparable to the FR deployment test using pressurized air (see section V.A.1). However, due to the slow build-up of pressure (15 min) to the level required for deployment (2 bar), the FR deployed slower using this test with heat transfer fluid than in the test with pressurized air.

The deployment satisfied the requirements: a maximum deflection angle (α) of less than $\pm$ 30° at a minimum pressure of 1,5 bar and deployment angle with the base-plane of the radiator (θ) of less than $\pm$ 45° (see Figure 18).

The thermal performance test on the RS was performed using the same setup (see Figure 19) as for the deployment test, however the air bearings in the hover disk were not pressurized (same as for thermal performance test, see section V.A.2). In addition, preventive measures were taken to prevent contamination of the facility by unforeseen fluid leaks. Furthermore, an optical cloth barrier was installed to enable taking IR images (see Figure 19).

Figure 18. Definition of deployment angle θ and deflection angle α

The system generated heat at the payload and transported the heat to the FR where the heat was dissipated to the environment by convection and radiation. The RS was subject to convective, radiative and conductive heat losses to the environment. Conductive loss in the PA was minimized by suspending the PA and conductive loss in the FRA was minimized by using a cork-based FRF and a low-conductive foil connection with the FRRS.

The FR temperatures were measured by means of T-Type thermocouples (see Figure 15 for thermocouple locations) and were used to correlate the numerical thermal model. Next, the numerical thermal model was used to determine the heat output with and without convective environment.

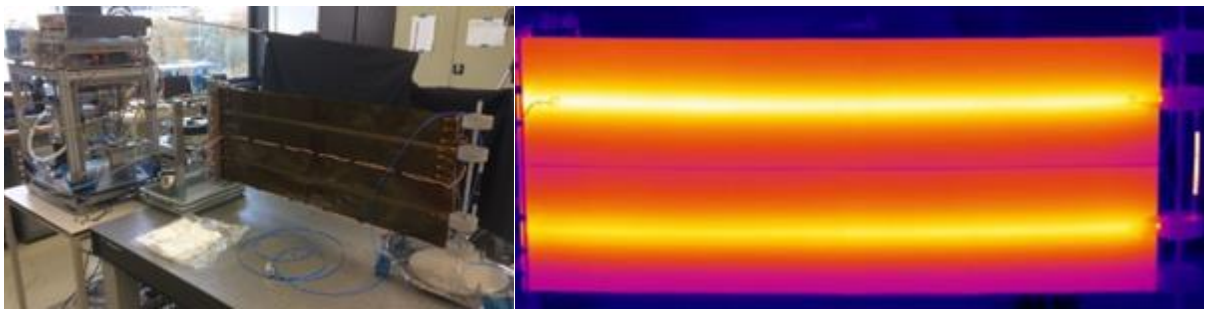

Figure 19. Thermal test setup (left), IR image of the functioning FR

The reference root temperature was 45 °C. The goal of the test was to determine the heat dissipation of the FR by measuring several performance indicators:

- Temperature difference between the FR fluid entrance and exit thermocouples
- Electrical power used by the payload ($Q_{payload}$)
- Temperature measurements at the PA fluid entrance and exit
- Average temperature of the FR

These performance indicators have been used to estimate the average convective and radiative power output of the FR, depending on the environment temperature. The temperature measurements on the PA were used to estimate the heat added by the PA (Q_{PA}). The thermocouples on the FR were used to correlate the numerical thermal model with the test results. The numerical thermal model was then adjusted to represent a space environment (vacuum and temperature of 2,7 K) and estimate the theoretical performance in space. The results are shown in Figure 20. The output of the numerical thermal model can be seen in Figure 21. From Figure 20 and Figure 21 it can be deduced that the total heat loss in the system (defined as all heat loss other than via the FR surface) is approximately 25-50 W.

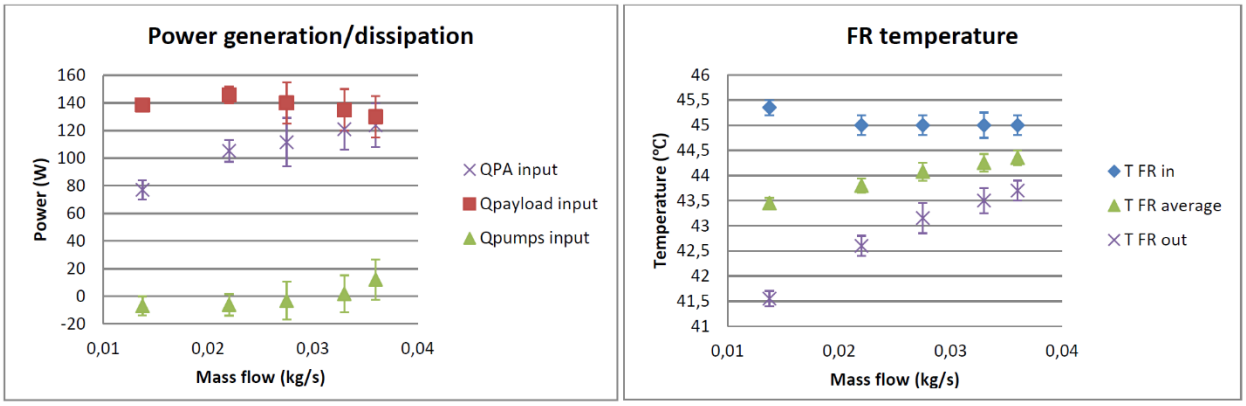

Figure 20. RS Thermal test results: heat transfers in the RS (left), FR temperatures (right)

The convective couplings and environmental temperature in the numerical thermal model were subsequently adjusted to estimate the thermal performance of the FR in a space environment (vacuum and temperature 2,7 K). The resulting heat dissipation in space was 240 W – 260 W. As a next step, the thermal numerical model uncertainties should be reduced (see section VI).

Two potential problems have been identified during the breadboard testing: vulnerability to MMOD and diffusion of Galden HT fluid through the tubing. These topics have been investigated in an additional small-scale breadboard test (see section V.B).

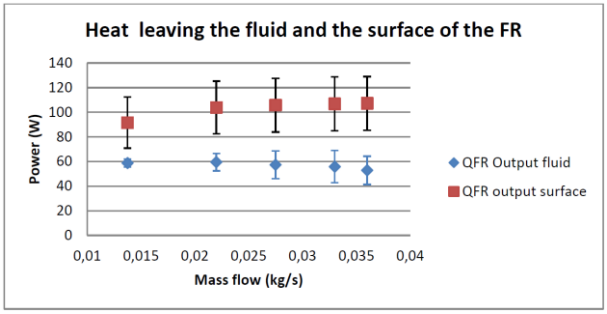

Figure 21. Heat output estimated by numerical thermal model correlation vs. mass flow

B. Lifetime Feasibility Analysis on FRA

This section provides the results of the assessment of expected lifetime in a geostationary space environment of the baseline INFRA concept (as described in section IV) and an adjusted/ruggedized design. Specifically, the following topics have been investigated:

1) Impact on the lifetime of the baseline design of permeation of Galden HT55 through kapton
2) Impact on the lifetime of the baseline design of Micro Meteoroid and Orbital Debris (MMOD)
3) Impact on the lifetime and performance of the baseline design of MMOD protection using bi-stable shielding

1. Impact on the lifetime of the baseline design of permeation of heat transfer fluid through kapton

The permeation of heat transfer fluid through the proposed kapton tubing is expected to be negligible based on literature research into permeability of kapton by noble gases. As shown in Figure 22, the molecule size is correlated with the breakthrough time of kapton film. More specifically, a molecule with an atomic diameter squared of approximately 20 $Å^2$ will take 300 years (10^{10} seconds) to break through a 50 µm thick kapton film. Galden HT55 heat transfer fluid has a molecule size of approximately 70 $Å^2$. Also, the results in Figure 22 were obtained using a wall thickness of 50,8 µm film rather than the 89 µm kapton tube wall thickness in the baseline INFRA design. For these two reasons, the breakthrough time is expected to be orders of magnitude larger than 300 years and therefore much larger the proposed lifetime of this radiator application (15 years).

2. Impact on lifetime of baseline design of MMOD

The fluid tubes in the baseline BB model of the FRA have been identified as the likely failure point due to MMOD. The fluid tubes were made from kapton and have a 6,35 mm inner diameter with a 0,089 mm wall thickness. Around the tube were layers of HiPeR laminate. Materials used in HiPeR other than kapton have a density and specific heat capacity similar to kapton, so it has been assumed that the entire thickness of the target (tube + laminate layers) was composed of kapton. The total thickness (270 ± 10 µm) has been reduced by 25% to account for slightly lower material strength than kapton. Refer to section IV.C for details on the FRA.

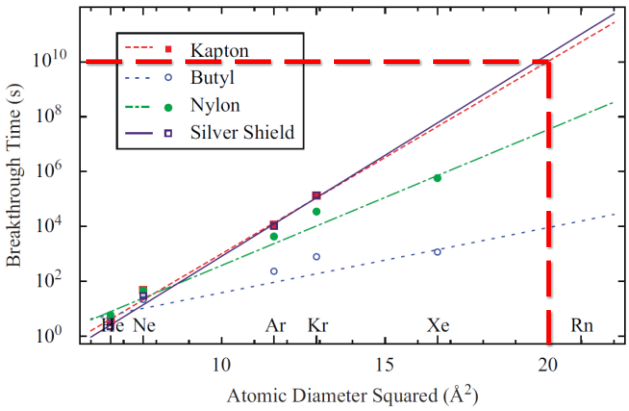

Figure 22. Breakthrough time vs. atomic diameter squared for 2 mil (50,8 µm) thickness materials[7]

Firstly, the baseline concept of bare kapton fluid tubing was assessed for susceptibility to fatal MMOD impact. Using area of the kapton tubing of the breadboard model (approximately 0,028 m^2) as input, Multiple Ballistic Limit Models (BLM) and MMOD models all predicted at least 20 fatal impacts over the design life of 15 years. Assuming an even distribution of fatal impacts over time, this indicated a fatal impact occurring within 1 year of service (see Table 3).

Table 3. Fatal impacts over 15 year design life of the INFRA radiator using several BLM and MMOD models.

	Projectiles with $m > 1{\cdot}10^{-9}$ g		Projectiles with $m > 1{\cdot}10^{-10}$ g	
Model	**Fatal impacts after 15 years**	**Duration until first fatal impact**	**Fatal impacts after 15 years**	**Duration until first fatal impact**
Divine (graphical)	49	0,3 years	80	0,2 years
DRAMA 2.2.0 (software)†	25	0,6 years	25	0,6 years
ECSS (equation)	37	0,4 years	79	0,2 years
Ekstrand (graphical)	20	0,8 years	123	0,1 years
Grun (equation)	56	0,3 years	134	0,1 years
Grun (graphical)	39	0,4 years	123	0,1 years
MASTER Data	59	0,3 years	147	0,1 years

† DRAMA indicated zero fatal impacts of the Kapton tubing for projectiles with mass below $1{\cdot}10^{-9}$ g.

Using the BLMs a minimum wall thickness for kapton, aluminium and stainless steel was determined for a Probability of No Penetration (PNP) of 0,90 and 0,95 (see Table 4). Results have been obtained using DRAMA/MIDAS software and its built-in thin-wall Cour-Palais ballistic limit equation.

Table 4. Minimum tube wall thickness required for PNP > 0,90 and > 0,95 for a kapton, aluminium and steel.

Shield/Wall Material	Material Density	Thickness for PNP > 0,90 after 15 years	Thickness for PNP > 0,95 after 15 years
kapton	1,4 g/cm^3	1,20 mm	1,65 mm
Aluminium	2,7 g/cm^3	0,80 mm	1,15 mm
Stainless steel	7,5 g/cm^3	0,45 mm	0,67 mm

It should be noted that the results in Table 3 and Table 4 have been obtained using tools and equations intended for much larger structures than INFRA and primarily for metallic shield walls. Conservative parameters have been chosen wherever appropriate.

3. Impact on the lifetime and performance of the baseline design of MMOD protection using bi-stable shielding

To ensure a satisfactory PNP several shielding concepts have been assessed: thicker kapton, aluminium bi-stable shield, steel bi-stable shield, braided stainless steel hose, dual bi-stable shield and fixed tubing. The steel bi-stable shield was selected as the most attractive concept based on a trade-off on mass, cost, thermal performance, shielding and stowed volume. This concept was subsequently detailed as the first shield layer connected to the kapton tube, followed by HiPeR laminate and further shielding.

To achieve the desired lifetime a steel shield thickness of 450 µm (0,45 mm) would be required (see Table 4) which has been arranged in 3 shield layers of 150 µm each (see Figure 23). This is a conservative estimate because the kapton layers, tubing and HiPeR laminate were not included in the analysis, but will likely also contribute to MMOD resistance. A breadboard assembly has been created that reliably self-deployed without damaging the kapton tubing or shielding. Bi-metallic material from a commercial tape measure (with coating removed) has been used.

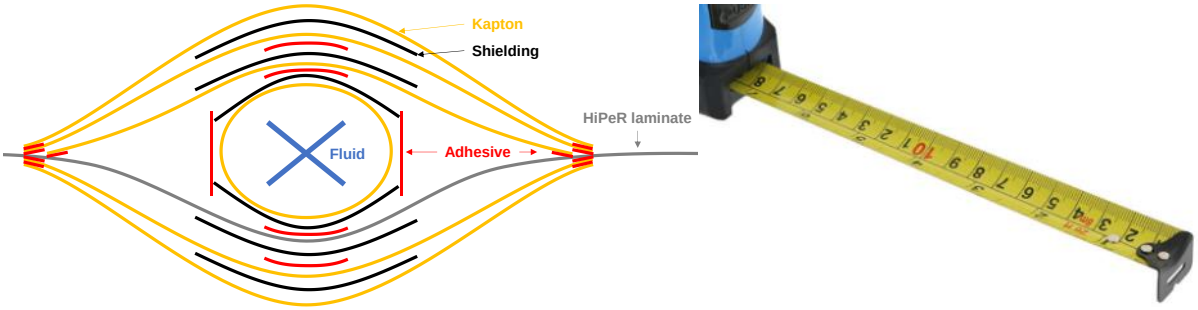

Figure 23. (left, not to scale) Indicative cross-section of the selected MMOD shielding arrangement. (right) Example of steel bi-stable material in a commercial tape measure (similar to material used in breadboard).

Images of the deployment are shown in Figure 24. The time from release to full deployment was approximately 0,8 seconds. This breadboard test was conducted with an 800 mm long single tube-and-shield arrangement without an extending laminate. The bends in part 1 to 4 of Figure 24 coincide with shield segment overlaps that were intentionally included to prevent local buckling.

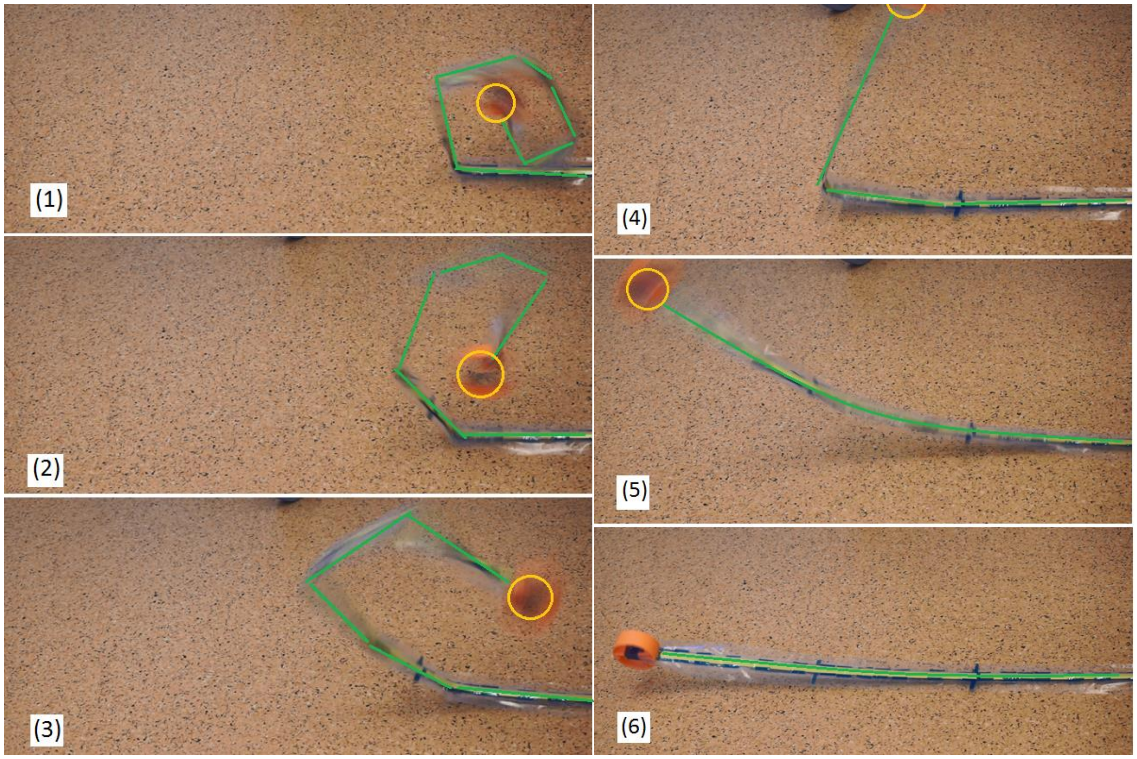

Figure 24. Images from a breadboard deployment of a single tube-and-shield.

The thermal performance compared to the baseline design was tested in a breadboard experiment. A 0,2 m by 0,2 m section of the FRA was used with MMOD shielding in place and heated water pumped through the kapton tube. The results (see Figure 25 for an impression) have a large uncertainty and are therefore not included in this paper.

The results did (as expected) indicate a degradation of thermal performance when compared to both the numerical thermal model as well as the thermal performance for the baseline INFRA breadboard model (see section V.A.3). As a consequence of adding shielding, the thermal performance, mass and stowed volume of the FRA were adversely affected as follows:

- Thermal impact: approximately 25-50%
- Mass impact: approximately 20-30%
- Volume impact (stowed): approximately 10-20%

It is deemed that the degradation can be strongly reduced by mitigation manufacturing immaturities in the design.

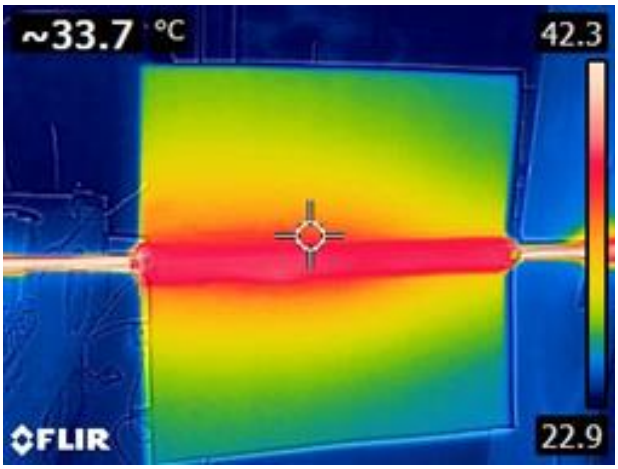

Figure 25. IR image from the thermal performance test of the INFRA design with MMOD shielding

An improved shielding arrangement is recommended (see Figure 26) based on the experience with testing the design as described above. A number of features are worth highlighting (reference in Figure 26):

1. To optimize the interface between the kapton tube and shielding, the inner shielding layer is narrower than the outer layers.
2. To increase stability during and after deployment, the two inner shield elements are fixed together with adhesive tape. To prevent buckling, the outer shield elements are free to move relative to the radiator.
3. To keep the shielding in place during and after deployment, adhesive tape is applied to the outer kapton sleeve layers. To increase heat transfer, kapton could be replaced with HiPeR laminate.
4. To optimize conductance, the kapton inner tube is connected to the inner shield layer with adhesive tape.
5. To optimize conductance, the HiPeR laminate is connected to the inner shield layer with adhesive tape.

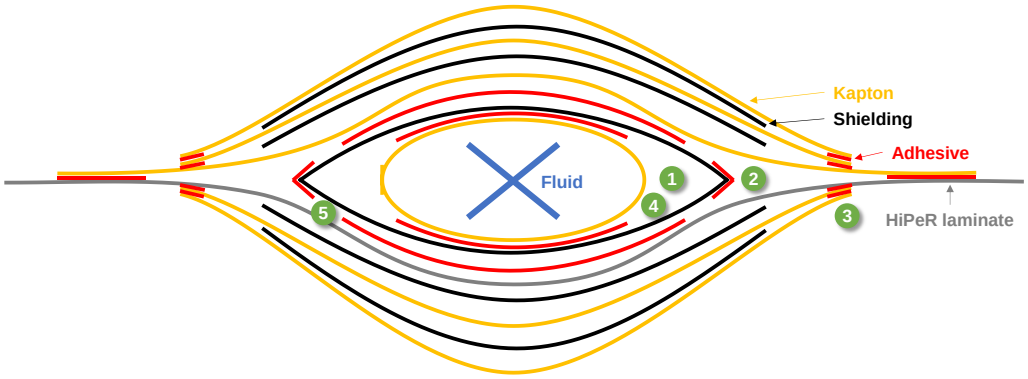

Figure 26. Cross-section of recommended improved MMOD shielding for INFRA (not to scale)

VI. INFRA Future Development

The following development areas have been identified to enhance the INFRA concept:

- Mass: the breadboard design is deemed promising, however an optimization is needed to achieve the target mass-to-power ratio, such as replacing metal parts (FRRS/HDRM/FRF) with a lighter material
- Retractability: investigate feasibility of making INFRA retractable, to reduce damage risk during high-thrust manoeuvres or MMOD
- Ease of integration: replace current BB supporting structure with design suitable for integration with (honeycomb) spacecraft wall
- Complexity reduction of PA: replace mini gear-pumps with multi-parallel micro-pumps
- MMOD shielding: reduce adverse impact, e.g. with thinner shield layers or improved manufacturing methods
- Verification: verify white paint integrity after rolling, test full scale model for deployment and thermal performance in vacuum (heat rejection by radiation only)

VII. Conclusion

Currently, the payload capacity of satellites is starting to become limited by their heat rejection capability, which is typically constrained by the exterior surface area of the spacecraft. The INFRA concept offers an extended surface for heat rejection, in combination with a compact stowed volume that can conveniently be placed alongside other appendages (e.g., solar arrays, antenna reflectors). The proposed INFRA concept consists of a HiPeR radiator and a single phase fluid loop. The flexible fluid tubing has two functions: deployment of the radiator (by increasing pressure) and heat transport. Based on the measured data, the thermal performance of an INFRA system operating at a 45 °C root temperature in a space environment with a sink temperature of -270 °C would be approximately 300-325 W/m^2. This corresponds to a radiator efficiency of approximately 60%. This performance is deemed to be competitive, especially considering the mass-to-power ratio (expected <10 kg / kW after a design iteration) and small stowed volume of such a system.

The permeation of heat-transfer fluid through the proposed kapton tubing is expected to be negligible. However, the fluid tubing is identified as the likely failure point due to MMOD: multiple models predict a fatal impact within 1 year of service. A revised design is proposed, with additional MMOD shielding in the form of bi-stable metal strips. The revised design results in a probability of no penetration of the kapton fluid tubing of 0,9 over a lifetime of 15 years. A small-scale breadboard test of the revised design has yielded promising results: successful deployment and a

first impression of the thermal performance. As expected, the adverse effects of this initial MMOD shielding arrangement are substantial: estimated thermal impact 25-50%, mass impact 20-30% and stowed volume 10-20%. However, a proposed improved shielding arrangement is expected to reduce these adverse effects and there is ample room for optimization of manufacturing methods.

Acknowledgments

The authors would like to acknowledge the significant contributions of Thomas Mason during his internship at Airbus DS NL and Carlo Pelt during his internship at NLR.

References

[1]Benthem, B., Airbus Defence and Space Netherlands B.V., Leiden, The Netherlands, European Patent Application for a "Radiator, as well as space vehicle structure comprising such radiator", EP2907757A1, filed 13 Jan. 2015.

[2]Benthem, B. and Mena, F., "Innovative new High Performance Radiators: Developing Heat Rejection Systems with Flexible Film Technology", *45th International Conference on Environmental Systems*, ICES-2015-180, Seattle, Washington, USA, 2015.

[3]Maas, A., "Development of Pyrolytic Graphite Applications in Spacecraft Thermal Control Systems", *47th International Conference on Environmental Systems*, ICES-2017-107, Charleston, South Carolina, USA, 2017.

[4]Gerner, H.J. van, Benthem, R.C. van, Es, J. van, "Fluid selection for space thermal control systems"; *44th International Conference on Environmental Systems (ICES)*, ICES-2014-136, Tucson, Arizona, USA, 2014

[5]Benthem, R.C. van, Es, J. van, Gerner, H.J. van, Vliet, A. van, Put, P. van, Schwaller, D., "Valve-less Mechanically Pumped Fluid Loop (MPFL) using East and West Panels of a Large Telecommunication Satellite as Radiator", *45th International Conference on Environmental Systems (ICES)*, ICES-2015-57, Seattle, Washington, USA, 2015

[6]Es, J. van, Gerner, H.J. van, Benthem, R.C. van, Lapensée, S., Schwaller, D. "Component Developments in Europe for Mechanically Pumped Loop Systems (MPLs) for Cooling Applications in Space", *46th International Conference on Environmental Systems*, ICES-2016-196, Vienna, Austria, 2016

[7]Schowalter, J. (2010), "Permeability of Noble Phases through kapton, Butyl, Nylon and Silver Shield", *Nuclear Instruments and methods in Physics Research A*, 615, 267-271